Interplanetary Consequences of a Large CME

M. Lahkar[1,2], P. K. Manoharan[2], K. Mahalakshmi[2], K. Prabhu[2], G. Agalya[2], S. Shaheda Begum[2], and P. Revathi[2]

[1] Centre for Radio Astronomy, Department of Physics, Cotton College, Guwahati, Assam, India
[2] Radio Astronomy Centre, National Centre for Radio Astrophysics, Tata Institute of Fundamental Research, Udhagamandalam (Ooty), India

Summary. We analyze a coronal mass ejection (CME) which resulted from an intense flare in active region AR486 on November 4, 2003. The CME propagation and speed are studied with interplanetary scintillation images, near-Earth space mission data, and Ulysses measurements. Together, these diverse diagnostics suggest that the internal magnetic energy of the CME determines its interplanetary consequences.

1 Introduction: intense flare and CME

An intense flare and associated coronal mass ejection (CME) occurred on November 4, 2003, during 19:50–20:10 UT in active region AR486. The onset of the halo CME was observed in the SOHO/LASCO C2 field of view (Brueckner et al. 1995) at 19:54 UT. The CME propagated rather fast in the C2–C3 field of view, at about 2650 km s^{-1} linear speed (Fig. 1), and caught up with a preceding CME that originated at the same location at 12:54 UT but had much lower linear speed (about 600 km s^{-1}) and narrow sky-plane width (about 70°). The LASCO images show interaction of the two CMEs at

Fig. 1. LASCO images showing CME–CME interaction

about $25R_{\odot}$. It caused remarkably complex and intense radio emission (e.g., Gopalswamy et al. 2001).

2 Radio spectra, particle fluxes, and scintillation images

Prior to the CME-CME interaction, intense type-III bursts were observed with space missions Wind, Cassini (Kliore et al. 2004), and Ulysses. In the WAVES spectrum (Bougeret et al. 1995), a fast-drifting intense type-II burst was observed during 19:50–21:00 UT at frequencies 1–11 MHz. It arrived at 1 MHz around 20:45 UT, corresponding to $R = 10 - 15R_{\odot}$ in good agreement with the LASCO data.

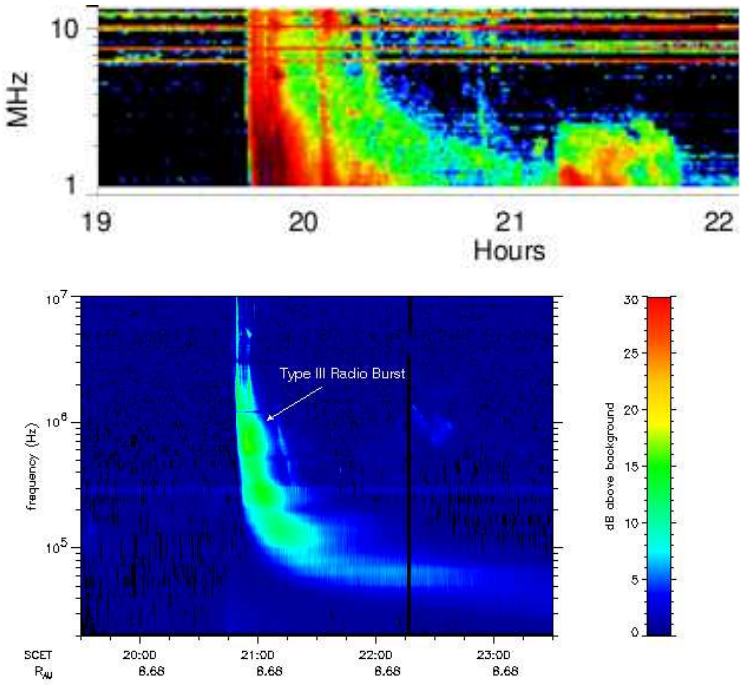

Fig. 2. Radio spectra from the WAVES and Cassini missions. Cassini was located at 8.7 AU.

The WAVES spectrum shows emission from the CME–CME interaction in the frequency range 1–3 MHz, higher than the type-II frequency at that time. Thus, this emission relates to about 15 times higher density than the typical ambient density at the interaction height (e.g., Gopalswamy et al. 2001). In the Cassini spectrum, an intense patch of emission occurred at frequencies below 1 MHz as the extension of the complex emission seen in WAVES. Thus, the

interaction led to electron acceleration through the intense magnetic field and reconnection resulting from the interaction. The interaction and associated phenomena were observed more than 30 minutes on the above radio spectra (Fig. 2).

Type-IV emission was observed at frequencies > 7 MHz during 20:10–21:00 UT (WAVES spectrum in Fig. 2) suggesting a plasmoid associated with the fast-moving CME (e.g., Manoharan & Kundu 2003). However, it disappeared just before the interaction.

The particle flux in the energy range 1–100 MeV showed no enhancement during the flare, but around 21:30 UT it increased in all energy bands to peak at about 06:00 UT the next day. Figure 3 shows that the increase was about 50 times above the pre-flare value at energies above 5 MeV. The sudden increase suggests that the CME-CME interaction favoured development of magnetic connectivity with the Earth and particle acceleration (e.g., Gargate et al. 2006). The CME-produced shock arrived on November 6, 19:20 UT (1-MeV profile in Fig. 3).

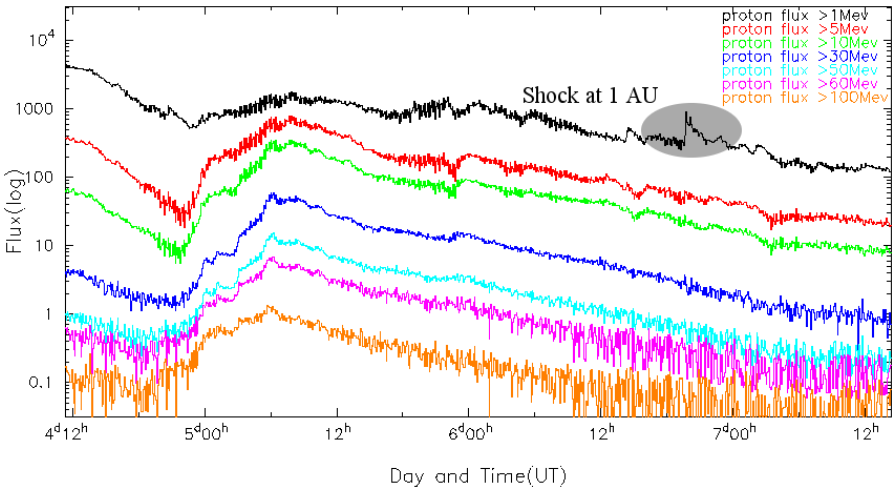

Fig. 3. Particle profiles in different energy bands.

Figure 4 shows 3-d tomographic interplanetary scintillation (IPS) images of the CME obtained with the Ooty Radio Telescope (e.g., Manoharan et al. 2001). They cover a range of 50–250 $R_{\odot}$. The interacting CMEs compressed the high-density and low-speed solar wind originating above a current sheet along the North-South direction. The IPS images obtained during November 6, 18:00–24:00 UT show the pushing and opening of the current sheet as viewed from the Earth. The central part of the CME compressed the fast solar wind belonging to a large coronal hole, which deflected the CME further away from the Sun-Earth line.

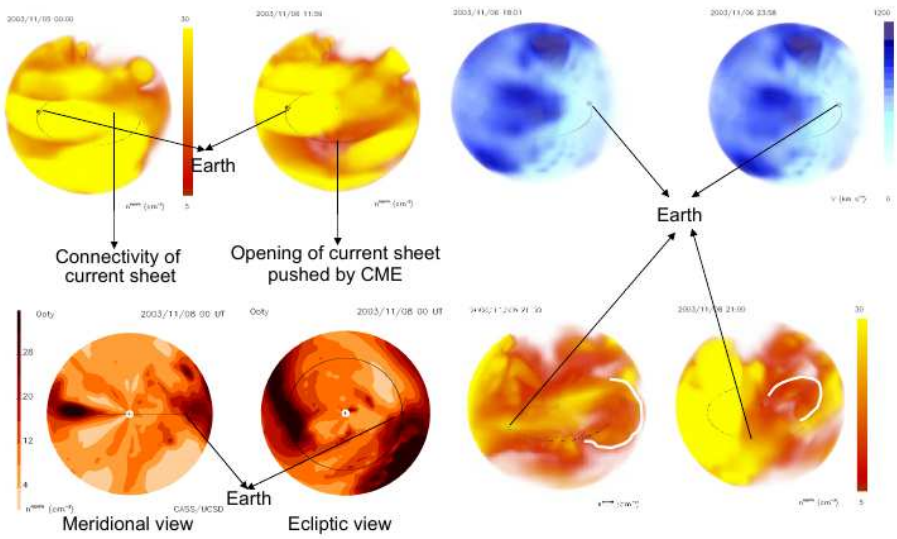

Fig. 4. Ooty IPS images showing the current sheet location (top left), CME deflection by the coronal hole (top right), CME compression of the solar wind (bottom left), and CME propagation (bottom right). The Sun is located at the center of each image. The two images at top right represent solar-wind speed; the others represent density.

The solar wind parameters observed by near-Earth and with the Ulysses space missions are shown in Fig. 5. The shock arrival times are shown by vertical lines. Since Ulysses was favourably located in the CME propagation direction, it could record the nose part of the CME and its shock, as indicated by a speed value of over 900 km s^{-1} at 5 AU. At Earth, the shock speed was below 600 km s^{-1}, suggesting that the eastern tail swept the Earth. From these measurements we infer a speed profile $V \sim R^{-0.4}$ to Earth. However, the deceleration $V \sim R^{-0.2}$ out to 5 AU near Ulysses implies gradual decline in speed along the CME propagation direction, which is in good agreement with the IPS measurements.

3 Conclusion

Our study shows the characteristics of a fast-moving CME and its interactions with transient and solar-wind structures at different distances from the Sun with good consistency between diverse diagnostics. The enhancement in radio emission and production of high-energy particles suggest that the magnetic field associated with the CME was strong. The gradual decline in CME speed suggests that the internal magnetic energy of the CME supported its prop-

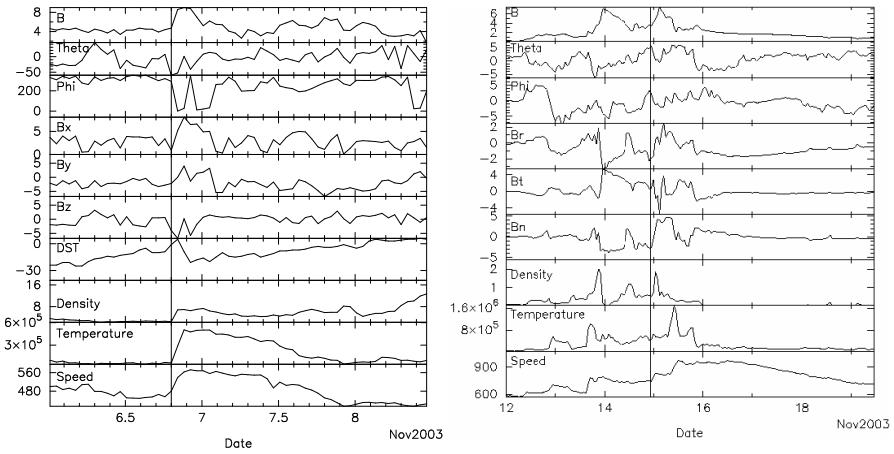

Fig. 5. 1-AU and Ulysses hourly averages of solar wind parameters.

agation including expansion in overcoming the aerodynamical drag imposed by the ambient solar wind (e.g., Manoharan 2006).

Acknowledgement. We thank the Cassini, GOES, SOHO, TRACE, Ulysses, Wind, and OMNI-database teams for making their data available on the web. We also thank B. Jackson and the UCSD team for the IPS tomography analysis package. M. Lahkar thanks the National Centre for Radio Astrophysics (TIFR) for financial support. This work is partially supported by the CAWSES–India program sponsored by the Indian Space Research Organisation (ISRO).

References

Bougeret, J.-L., Kaiser, M. L., Kellogg, P. J., et al. 1995, Space Sci. Rev., 71, 231
Brueckner, G. E., Howard, R. A., Koomen, M. J., et al. 1995, Solar Phys., 162, 357
Gargate, L., Bingham, R., Fonseca, R. A., Silva, L. O. 2006, AGU Fall Meeting Abstracts, B1518
Gopalswamy, N., Yashiro, S., Kaiser, M. L., Howard, R. A., Bougeret, J.-L. 2001, ApJ, 548, L91
Kliore, A. J., Anderson, J. D., Armstrong, J. W., et al. 2004, Space Sci. Rev., 115, 1
Manoharan, P. K. 2006, Solar Phys., 235, 345
Manoharan, P. K., Kundu, M. R. 2003, ApJ, 592, 597
Manoharan, P. K., Tokumaru, M., Pick, M., et al. 2001, ApJ, 559, 1180